On PKM with Articulated Travelling-Plate and Large Tilting Angles

François Pierrot, Olivier Company, Sébastien Krut

On PKM with Articulated Travelling-Plate and Large Tilting Angles

François Pierrot, Olivier Company, Sébastien Krut

LIRMM, UMR 5506 CNRS – Université Montpellier 2
161 rue Ada, 34392 Montpellier CEDEX 5, France
pierrot@lirmm.fr

1 Abstract

This paper discusses some ways to achieve large tilting motions with PKM by resorting to articulated travelling plate. Different known options are firstly presented: remote actuation, hybrid architectures, redundancy, rotation amplification and translation-to-rotation transformation.

Starting from two of those features, the aim of this paper is to go one step further and to propose two ideas:

(1) It might be indeed possible to obtain a 4-dof design which compares directly with commercially available Delta-based robots (*e.g.* the FlexPicker, an ABB Robotics equipment) in terms of technology, workspace, and performance while avoiding the ***R****UPUR* kinematic chain.

(2) It might be possible to design a 5-dof machine with large tilting angle about two axes.

2 Introduction

The idea of parallel mechanisms resorting to a non-rigid (or: *articulated*) moving platform which includes passive joints has been introduced recently and a few academic prototypes have already demonstrated the effectiveness of this principle [3] [7] implemented for Scara motions. Indeed, the 4 *dof*[1] of Scara motions are well adapted to pick-and-place tasks: 3 translations to carry an object from one point to another, plus one 360-degreerotation about a given axis in world coordinates for the orientation. Robots inspired from Delta [1] architecture encountered a real commercial success achieving this task because of their high dynamics. This is due to the lightweight (actuators are fixed on the base) parallel (having closed kinematics chains) design. However, the ***R****UPUR* kinematic chain (*R*: Revolute, *U*: Universal, *P*: Prismatic, bold letter stands for actuated joint)) that transmits the rotational motion from a revolute actuator fixed on the frame to the effector (see Figure 1) may become a weak point. This is particularly true for Delta with huge workspace or, even more, with linear Delta that might be used for designing machine-tools.

Most of recent researches in that field have proposed different designs for obtaining Scara motions either for serving as pick-and-place robots, or for being a part of a more complex machine-tool; some of them are parallel mechanisms, like Kanuk [2] or H4 [3], some others have non-fully-parallel designs [4]. Other four-dof parallel mechanisms have been studied in the past, but they are dedicated to different applications such as Koevermans' flight simulator [5] and Reboulet's four-dof wrist [6]. Even more recently, a machine with a moving platform including passive prismatic joints and a "Translation-to-Rotation" transformation system has been introduced [7]; in the later paper it was shown that for a very specific design ((i) four linear motors in the same plane and aligned on the same direction, (ii) a three-part moving platform) it was possible to get a realistic practical design and very simple kinematics model in closed form for both Inverse and Forward problems.

The aim of this paper is to go one step further and to propose two ideas:

(3) It might be indeed possible to obtain a 4-dof design which compares directly with commercially available Delta-based robots (*e.g.* the FlexPicker, an ABB Robotics equipment) in terms of technology, workspace, and performance while avoiding the ***R****UPUR* kinematic chain.

(4) It might be possible to design a 5-dof machine with large tilting angle about two axis.

To do so, we have designed a prototype of a machine we called I4R by resorting to several components from FlexPicker. In this paper, this prototype is described and the way to achieve the desired rotation is discussed. Then, geometrical models are derived (a nice feature for this robot is that the forward geometrical model can be written in a closed form). Afterward, a kinematic modelling able to witness to all the singularities of the robot is established: this is based on a detailed modelling of the so-called "spatial parallelograms" which are described here for what they really are (two *SS* chains). It shows up the geometrical condition that must be validated in order to get the desired motions.

Moreover, we present here an "extension" of this principle (an articulated travelling plate with a passive linear joint) by combining it with actuation redundancy so that we obtain a 5-dof, large-tilting-angle solution.

[1] dof: degree of freedom

3 Getting large tilting angles

It is well established that PKM suffer from different types of singularities that are often said to belong to two families:

- Serial-type (or under-mobility) when the mechanism looses one (or more) degree of freedom;
- Parallel-type (or over-mobility) when the mechanism's stiffness vanishes in one (or more) direction.

This paper will later discuss this description of singularities (even explaining that additional problems exist …) but it is nevertheless true that the tilting angle is often limited by parallel-type singularities. So far, different solutions have been proposed to overcome that problem and getting larger tilting angle, as described in the following sub-sections.

3.1 Remote actuation

One way to get large tilting angle is to arrange one revolute joint on the travelling plate (in a "serial" way) and, to limit the moving parts masses, to place the actuation in a remote location, that is, the base. It is the option selected for most Delta robots, as in Figure 1 which shows the telescopic fourth chain (with an RUPUR arrangement) dedicated to the tool rotation. This principle allows the rotation range to be as large as for serial chains (indeed, the last rotation is actually arranged in a serial way ...) while keeping the moving masses low because the motors is still fixed on the base.

Figure 1. ABB Robotics FlexPicker with its remote actuation.

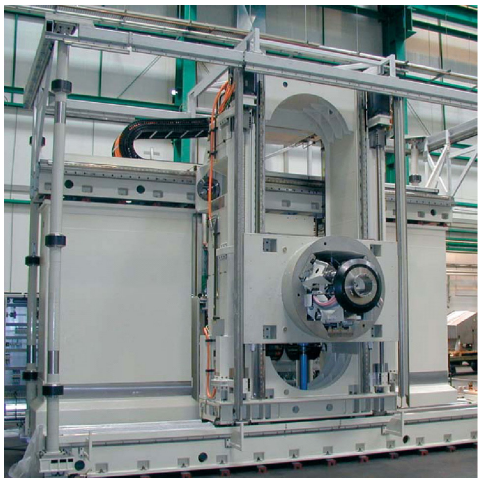

Figure 2. An hybrid machine by DS Technologies

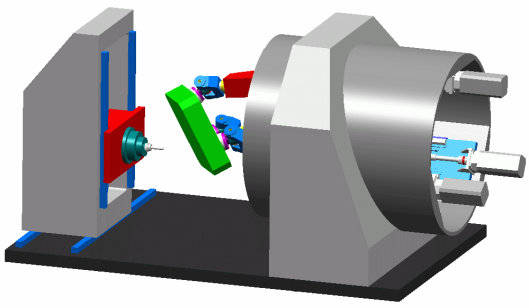

Figure 3. An example of Left-hand / Right-hand concept.

Figure 4. Speed-R-Man, a kinematically redundant PKM.

3.2 Hybrid architectures

Kinematic optimisation is always an opened option when a PKM has to be designed, and it is often feasible to select an "optimal" set of design parameters (position of actuators, length of legs, etc.) to maximise the workspace of a mechanism in terms of tilting angle range. Obviously, this optimisation process is made easier if some constraints are removed, for example if the machine is designed for tilting purpose only.

This solution leads to machines made with two sub-parts, each of them specialized in part of the task, *e.g.*:

- An X-Y serial machine can carry a Z-A-B PKM module, this module carrying the spindle and offering a larger-than-usual tilting range (Figure 2);
- One part of the machine carries the spindle, while the part is moved by another sub-part, following the robotics "left-hand/right-hand" concept. Again the PKM module may easily be optimised for large tilting angle (Figure 3).

3.3 Redundancy

The general concept of "redundancy" applied to mechanism theory can be roughly stated as follows: installing more actuators than the number of the TCP's degrees of freedom. For serial chains, this gives, for a given position of the TCP, and infinite number of actuated joints positions. Selecting properly a set of joints position may help in avoiding singularities. This option (called "kinematic redundancy") exists for PKM but it has been used in a very limited numbers of cases (Figure 4 shows one example of such an arrangement). The principle is here to select among the possible joint positions, one position that is far enough from singularities.

Moreover, PKM offer the ability to create a different type of redundancy, called "actuation redundancy", that can be described as follows: for a given set of external load, an infinite number of joint force sets exist for balancing the external load. In that case, the principle is to choose among the possible set of joint forces, one set of forces which guarantees a good stiffness (see [16] for a good implementation of such a principle).

This type of redundancy has been studied in more details for PKM than the previous one (for kinematic redundancy most efforts had been dedicated to the serial case) and several prototypes have been built, giving researchers the opportunity to evaluate control schemes. Indeed, control is here the key issue since actuation redundancy leads to over-constraint mechanisms; consequently internal forces may exist, and control schemes have to cope with that. We have, for example, done such works on a 3-dof test bed called Archi (see Figure 5).

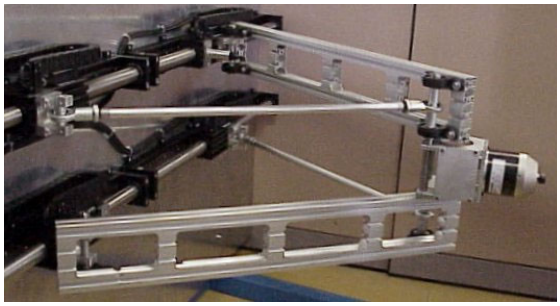

Figure 5. Archi: a 3-dof, 4-motors, actuation-redundant PKM.

3.4 Rotation amplification

In recent years, we have studied such an option in some details, by proposing different mechanisms architectures based on one key principle: designing a travelling plate which includes passive revolute joints. This was the base of H4 architecture, a mechanism for "Scara-like motion", that is XYZ translation, plus a rotation about Z axis. As depicted in Figure 5 and Figure 6, H4 is based on 4 identical elementary chains ($R[SS]_2$ chains) and a travelling plate equipped with 3 passive revolute joints. The last revolute joint is moved by a coupling system about a 360-deg range, which related its motion to the motion of another passive revolute joint that has only a 90-deg range.

Moreover, we have studied the principle of rotation amplification about not only one axis, but *two* axes. Even though such ideas remain quite preliminary (none implementation have been tested so far), it shows that it might be possible to create mechanisms that could double a PKM traveling plate rotation about two axis: the Twice concept aims at such a result, and might be mounted on top of a classical PKM, *e.g.* in Figure 7, on a Delta.

3.5 Translation-to-Rotation transformation

It has been shown that H4 is an architecture providing Scara motions. One specific feature of this architecture is its articulated nacelle (made with two pivot joints) which is linked to the base by four identical Delta-like "spatial parallelograms". This nacelle can be equipped with an additional gear-based amplification system leading to a large and adjustable range of motion in orientation. However, some of its limitations can be pointed out:

- When the tool orientation changes, the Jacobean matrix condition number may vary a lot, leading to important changes in the machine behavior;
- It has been proved that the relative positions of the four "spatial parallelograms" must be properly selected to avoid singular cases;
- Its forward geometrical model has not been established in analytical form, except for specific arrangements.

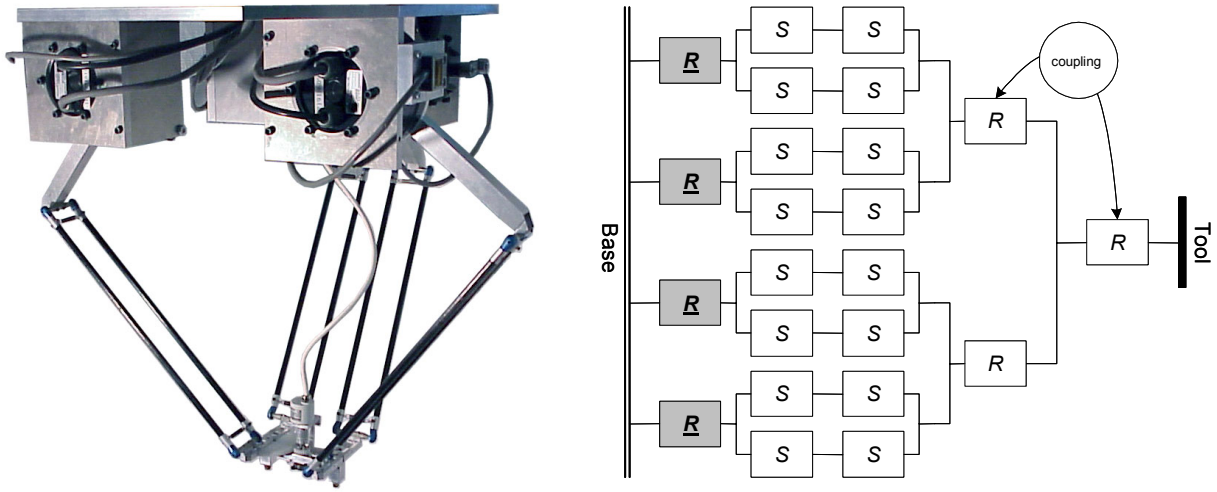

Figure 6. H4 robot: picture of actual prototype and kinematics graph showing the rotation amplification by a coupling system.

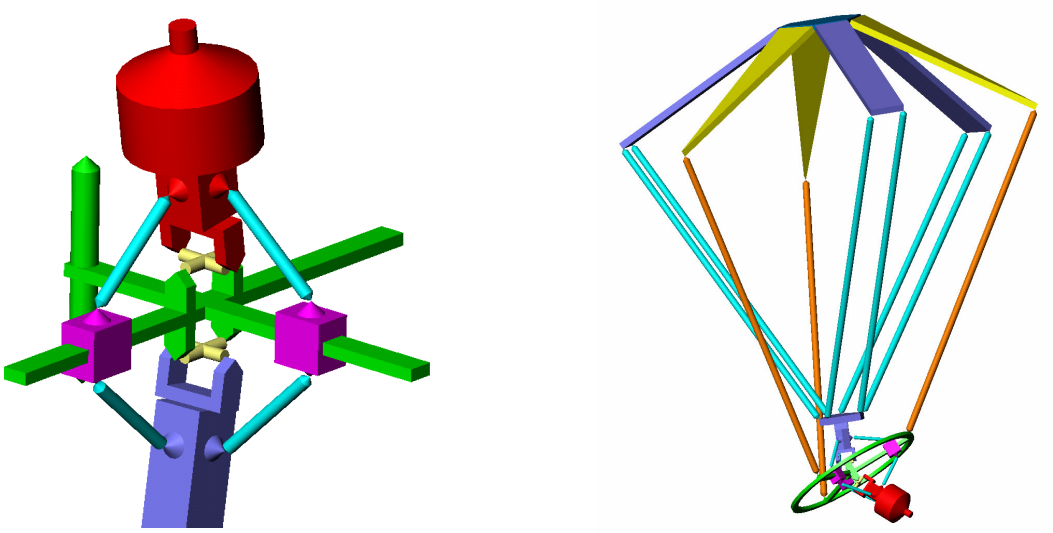

Figure 7. The Twice mechanism (left), where the spindle tilts twice as much as the travelling plate (the cross-shaped piece), might be mounted on a Delta machine (right).

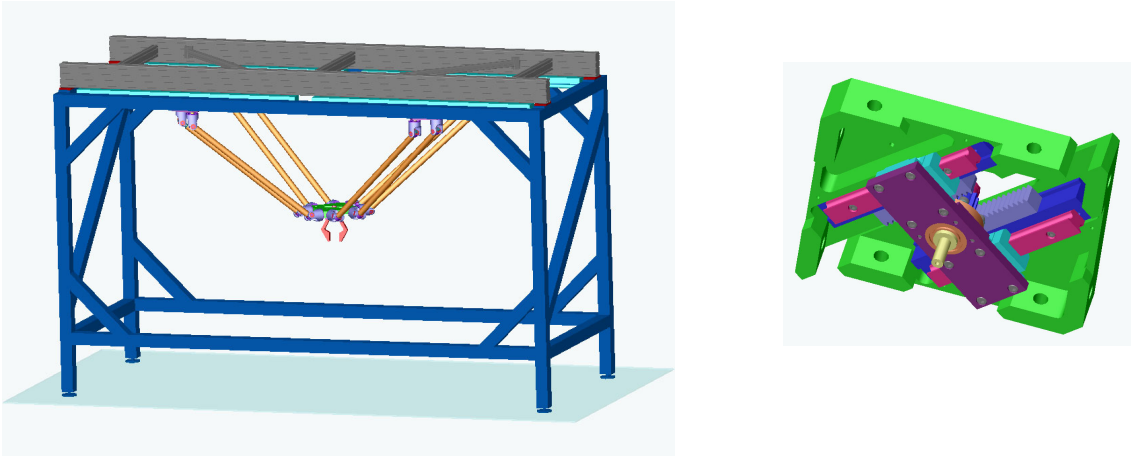

Figure 8. I4L: a first prototype with T-to-R transformation

It has been proposed (see Figure 8-left) to build traveling plates with *prismatic* passive joints instead of revolute joints. It is always possible to transform this translational motion into a rotative one by means of rack-and-pinion, belt, cable-and-pulley, … as shown in Figure 8-right. This solves most difficult points due to revolute joints: models are simpler, load balance is easier to achieve, general design is simpler, …

4 I4R: an efficient implementation of T-to-R transformation

This 4-dof design might compare directly with commercially available Delta-based robots.

4.1 Description of the prototype

The practical design is extremely simple thanks to the forearms and spatial parallelograms taken from the FlexPicker (see Figure 9, left hand side).

The main difference with the FlexPicker results in the use of 4 parallelograms instead of 3. Furthermore, instead of being rigid, the moving platform is articulated and does not require the kinematic chain transmitting the rotational motion to the end-effector. It is composed of two different parts (while the machine in [7] utilizes a three-part moving platform) linked together by a prismatic guide, plus a pulley-cable system which transforms the relative translation of both parts into the desired rotation (see Figure 9, right hand side).

It gives a workspace similar to FlexPicker's one – a 1-meter radius, 0.2-meter high cylinder – but overcomes the problems due to the effector's rotation. The brushless revolute actuators are associated to gear units with very low backlash (<1'). Moving parts are intended to be as light as possible: forearms and parallelograms are carbon fibre parts (from ABB Robotics), while the travelling plate is made of aluminium. The expected performances for this robot are: 100 [m/s2] acceleration and 10 [m/s] velocity (*Note: It is too early to guarantee that such performances will be reached, even though our first tests are encouraging*).

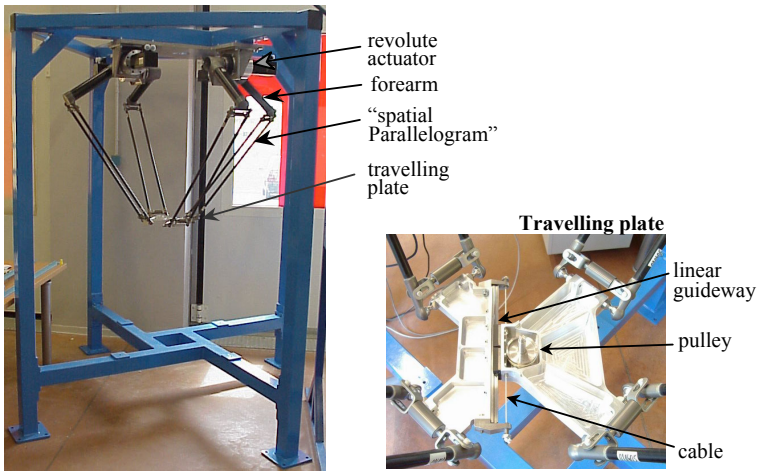

Figure 9. I4R prototype (left) and its travelling plate with a prismatic passive joint (right).

4.2 Basic modelling

In Figure 10, a joint-and-loop graph is depicted: grey boxes represent actuated joints, white boxes passive joints. Underlined letter stands for a joint equipped with sensors. Circles express a coupling between two joints. It is worth noting that this mechanism is, on one hand *under-constrained* (as for many Delta-like designs, each rod between two *S* joints can rotate about its own axis) and on the other hand, *over-constrained* (a Grübler analysis would show one degree of constraint). Figure 11 depicts the whole geometry of the mechanism.

* $\boldsymbol{x} = [x \quad y \quad z \quad \theta]^T$ is the generalized operational vector.

* $\boldsymbol{q} = [q_i]$ is the generalized joint vector. q_i are the joint coordinates (angles measured in planes $(\mathrm{P}_i, \vec{e}_z, \vec{e}_i)$ starting from $\vec{e}_z$).

* P_i[2], $i \in \{1,2,3,4\}$, represent the positions of the actuators:

$$\boldsymbol{P}_1 = [-e \quad -d \quad 0]^T, \boldsymbol{P}_2 = [e \quad -d \quad 0]^T, \tag{1}$$

$$\boldsymbol{P}_3 = [-e \quad d \quad 0]^T, \boldsymbol{P}_4 = [e \quad d \quad 0]^T, \tag{2}$$

* $\vec{u}_i$ characterizes the orientation of the forearms:

[2] Each geometrical vector $\vec{u}$ will be associated to a column vector $\boldsymbol{u}$ expressed in the canonic base $\mathcal{B} = (\vec{e}_x, \vec{e}_y, \vec{e}_z)$. Moreover, column vector $\boldsymbol{P}$ will represent geometrical point P in frame $\Re = \langle O, \mathcal{B} \rangle$.

$$\boldsymbol{u}_i = \left[\cos(\alpha_i) \quad \sin(\alpha_i) \quad 0\right]^T,\ i \in \{1,2,3,4\}, \tag{3}$$

where α_i are angles measured about $\vec{e}_z$ relatively to $\vec{e}_x$.

* A_i is the geometrical point located in the middle of A_{i1} and A_{i2} representing the spherical joints centres:

$$\boldsymbol{A}_i = \boldsymbol{P}_i + \boldsymbol{L}_i,\ i \in \{1,2,3,4\} \tag{4}$$

with:

$$\boldsymbol{L}_i = \left[L\sin(q_i)\cos(\alpha_i) \quad L\sin(q_i)\sin(\alpha_i) \quad L\cos(q_i)\right]^T, \tag{5}$$

where: L is the length of the bars.

* B_i is the geometrical point situated in the middle of B_{i1} and B_{i2} representing the centre of the spherical joints between the forearms and the moving platform:

$$\boldsymbol{B}_i = \boldsymbol{D} + k_i\,\theta\,\boldsymbol{v}_1 + \boldsymbol{E}_i,\ i \in \{1,2,3,4\}, \tag{6}$$

with:
$$k_1 = k_2 = R \text{ and } k_3 = k_4 = 0, \tag{7}$$

$$\boldsymbol{D} = \left[x \quad y \quad z\right]^T, \tag{8}$$

$$\boldsymbol{E}_1 = \left[-E \quad -D \quad 0\right]^T,\ \boldsymbol{E}_2 = \left[E \quad -D \quad 0\right]^T, \tag{9}$$

$$\boldsymbol{E}_3 = \left[-E \quad D \quad 0\right]^T,\ \boldsymbol{E}_4 = \left[E \quad D \quad 0\right]^T, \tag{10}$$

$$\boldsymbol{v}_1 = \boldsymbol{e}_x \tag{11}$$

($\boldsymbol{v}_1$ characterises the direction of the guide and R is the radius of the pulley: $t = R\theta$.)

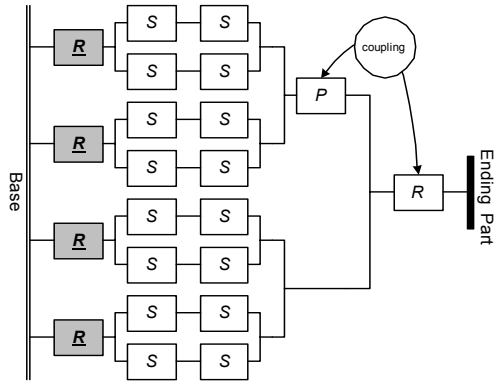

Figure 10. I4R's joint-and-loop graph

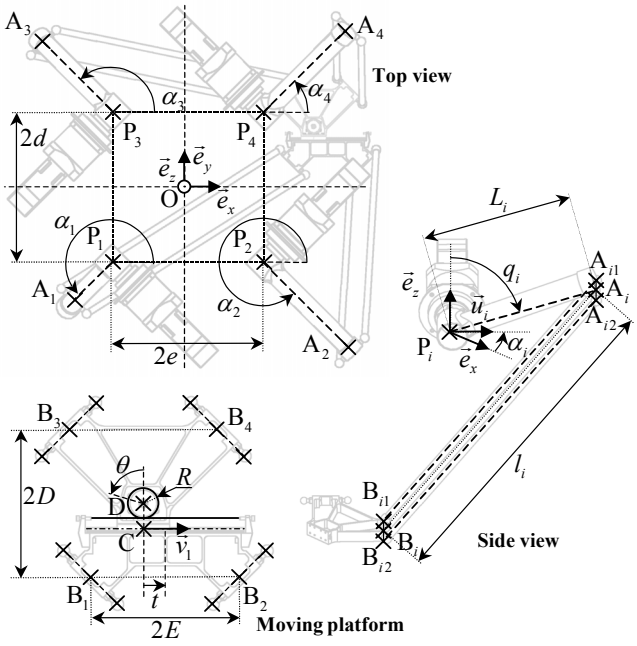

Figure 11. Geometrical modelling of the I4R structure

As it is usual for most parallel robots, the inverse position relationship is easy to derive from the following equality:

$$\left\|\boldsymbol{l}_i\right\| = l,\ i \in \{1,2,3,4\} \tag{12}$$

where $\boldsymbol{l}_i$ is the vector joining A_i to B_i ($\boldsymbol{l}_i = \boldsymbol{A}_i - \boldsymbol{B}_i$)

For this robot the resolution is derived for rotational motors as in [10] and leads to:

$$M_i\cos(q_i) + N_i\sin(q_i) = G_i,\ i \in \{1,2,3,4\} \tag{13}$$

where:
$$M_i = 2L(\boldsymbol{B}_i\boldsymbol{P}_i.\boldsymbol{e}_z),\ N_i = 2L(\boldsymbol{B}_i\boldsymbol{P}_i.\boldsymbol{u}_i), \tag{14}$$

$$G_i = l^2 + \left\| \boldsymbol{B}_i \boldsymbol{P}_i \right\|^2 - L^2 \ , \ \boldsymbol{B}_i \boldsymbol{P}_i = \boldsymbol{P}_i - \boldsymbol{B}_i \ . \tag{15}$$

($\boldsymbol{B}_i$ is given by relation (6) when knowing the operational coordinate vector. "**.**" represents a dot product).

Making the classical change of variable:

$$t_i = \tan(q_i / 2) \ , \tag{16}$$

leads to a second degree polynomial equation. Once solved, only the root corresponding to the realistic posture is kept, and the joint coordinates can be written as follow:

$$q_i = 2 \tan^{-1} \left(\frac{-b_i + \sqrt{b_i^2 - 4 a_i c_i}}{2 a_i} \right), \quad i \in \{1, 2, 3, 4\} \tag{17}$$

with a_i , b_i et c_i the polynomial coefficients:

$$a_i = G_i + M_i \ , \ b_i = -2 N_i \ \text{ and } \ c_i = G_i - M_i \ . \tag{18}$$

Note: the forward kinematic model can be derived in **closed** form too, but the derivation is not shown here for lack of space.

4.3 Singularity analysis

Singularities analysis is often based on analysis of the standard Jacobean matrices $\boldsymbol{J}_x$ and $\boldsymbol{J}_q$ representing the input-output velocity relationship:

$$\boldsymbol{J}_q \, \dot{\boldsymbol{q}} = \boldsymbol{J}_x \, \dot{\boldsymbol{x}} \ , \tag{19}$$

where $\dot{\boldsymbol{q}}$ and $\dot{\boldsymbol{x}}$ are respectively the joint velocity vector and the operational velocity vector.

But other kind of singularities can occur [8]. To enlighten them, a deeper analysis is required. At first, we will recall the fact that "spatial parallelograms" can be seen in two different ways, and that we consider here the realistic case where spherical joints are modelled as 3-dof joints and not 2-dof joints. Then, two types of modelling will be given: one suggesting that the linear guide is a cylindrical joint (isostatic modelling), and another assuming that it is a prismatic joint (over-constrained modelling). In both case, geometrical constraints, which must be fulfilled to get rid of internal singularities, will be derived.

4.3.1 Preliminary remark

According to Hervé's notations [13] for displacements subgroups, $\{T\}$ stands for the subgroup of spatial translations and $\{X(\mathbf{u})\}$ stands for the subgroup of Schoenflies displacements (or Scara motion), where $\mathbf{u}$ is a unitary vector collinear to the rotation's axis. If a closed loop mechanism is composed of two chains producing Schoenflies displacements with $\mathbf{v} \neq \mathbf{u}$, then:

$$\{X(\mathbf{u})\} \bigcap \{X(\mathbf{v})\} = \{T\}$$

that is to say that such a mechanism will produce only three translations. The case of machines with ***R****R(RR)*2*R* chains (Figure 12-a) is easily handled with such a technique since those chains correspond to Schoenflies subgroup.

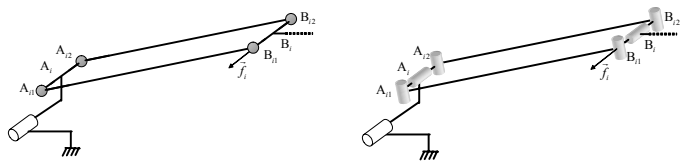

(a) P*(SS)2* (b) $\underline{\boldsymbol{P}}R(RR)_2 R$

Figure 12. Two ways to model "spatial parallelograms".

The case of machines with $\underline{\boldsymbol{R}}(SS)_2$ chains (Figure 12-b) is more complex: each chain provides 5 dof, 3T-2R, and does not correspond to a group. Indeed it is possible that the union ($\cup$) of two 3T-2R chains generates a 3T-3R motion. The following sub-sections consider precisely this type of $\underline{\boldsymbol{R}}(SS)_2$ chains.

4.3.2 Isostatic modelling

Here, the prismatic guide is represented by a *cylindrical joint* offering one degree of freedom in translation and one degree of freedom in rotation along the same axis. Such a hypothesis offers: (i) a number of internal dof consistent with a Grübler analysis (no internal constraint), (ii) a model of prismatic joint with very low torsional stiffness.

On the one hand, a 4-dof subset made of the actuators can be observed. On the other hand, an 8-dof travelling plate can be found: 3 for positioning, 3 for orientating, and 2 considering inter-part mobilities (the linear guide is represented by a 2-dof cylindrical joint). Single bars equipped with spherical joints separate both subsets. Each implies that the distance between their extremities is invariant:

$$\left\| \boldsymbol{l}_{ij} \right\| = l \ , \ i \in \{1,2,3,4\} \ , \ j \in \{1,2\} \ , \tag{20}$$

where $\boldsymbol{l}_{ij}$ is the vector joining A_{ij} to B_{ij} ($\boldsymbol{l}_{ij} = \boldsymbol{A}_{ij} - \boldsymbol{B}_{ij}$).

Deriving this relation leads to the "equiprojectivity" of velocities of the extremities of each rod:

$$\boldsymbol{v}_{\mathrm{A}_{ij}} . \boldsymbol{l}_{ij} = \boldsymbol{v}_{\mathrm{B}_{ij}} . \boldsymbol{l}_{ij} \ , \ i \in \{1,2,3,4\} \ , \ j \in \{1,2\} \ , \tag{21}$$

where $\boldsymbol{v}_{\mathrm{A}_{ij}}$ (respectively $\boldsymbol{v}_{\mathrm{B}_{ij}}$) represents the velocity of point A_{ij} (B_{ij}) relatively to the ground.

As a consequence, a linear system representing the whole kinematic of the mechanism can be derived when writing the "equiprojectivity" relations for the 8 rods:

$$\begin{bmatrix} \boldsymbol{r}_1.\boldsymbol{l}_{11} & 0 & 0 & 0 \\ \boldsymbol{r}_1.\boldsymbol{l}_{12} & 0 & 0 & 0 \\ 0 & \boldsymbol{r}_2.\boldsymbol{l}_{21} & 0 & 0 \\ 0 & \boldsymbol{r}_2.\boldsymbol{l}_{22} & 0 & 0 \\ 0 & 0 & \boldsymbol{r}_3.\boldsymbol{l}_{31} & 0 \\ 0 & 0 & \boldsymbol{r}_3.\boldsymbol{l}_{32} & 0 \\ 0 & 0 & 0 & \boldsymbol{r}_4.\boldsymbol{l}_{41} \\ 0 & 0 & 0 & \boldsymbol{r}_4.\boldsymbol{l}_{42} \end{bmatrix} \begin{bmatrix} \dot{q}_1 \\ \dot{q}_2 \\ \dot{q}_3 \\ \dot{q}_4 \end{bmatrix} = \begin{bmatrix} \boldsymbol{l}_{11}^{\ T} & R\boldsymbol{v}_1.\boldsymbol{l}_{11} & [\boldsymbol{e}_{11} \times \boldsymbol{l}_{11}]^T & (\boldsymbol{v}_1 \times \boldsymbol{d}_{11}).\boldsymbol{l}_{11} \\ \boldsymbol{l}_{12}^{\ T} & R\boldsymbol{v}_1.\boldsymbol{l}_{12} & [\boldsymbol{e}_{12} \times \boldsymbol{l}_{12}]^T & (\boldsymbol{v}_1 \times \boldsymbol{d}_{12}).\boldsymbol{l}_{12} \\ \boldsymbol{l}_{21}^{\ T} & R\boldsymbol{v}_1.\boldsymbol{l}_{21} & [\boldsymbol{e}_{21} \times \boldsymbol{l}_{21}]^T & (\boldsymbol{v}_1 \times \boldsymbol{d}_{21}).\boldsymbol{l}_{21} \\ \boldsymbol{l}_{22}^{\ T} & R\boldsymbol{v}_1.\boldsymbol{l}_{22} & [\boldsymbol{e}_{22} \times \boldsymbol{l}_{22}]^T & (\boldsymbol{v}_1 \times \boldsymbol{d}_{22}).\boldsymbol{l}_{22} \\ \boldsymbol{l}_{31}^{\ T} & 0 & [\boldsymbol{e}_{31} \times \boldsymbol{l}_{31}]^T & 0 \\ \boldsymbol{l}_{32}^{\ T} & 0 & [\boldsymbol{e}_{32} \times \boldsymbol{l}_{32}]^T & 0 \\ \boldsymbol{l}_{41}^{\ T} & 0 & [\boldsymbol{e}_{41} \times \boldsymbol{l}_{41}]^T & 0 \\ \boldsymbol{l}_{42}^{\ T} & 0 & [\boldsymbol{e}_{42} \times \boldsymbol{l}_{42}]^T & 0 \end{bmatrix} \begin{bmatrix} \dot{x} \\ \dot{y} \\ \dot{z} \\ \dot{\theta} \\ \omega_x \\ \omega_y \\ \omega_z \\ \dot{\varepsilon} \end{bmatrix} \tag{22}$$

Where

"$\times$" represents the cross product

$\boldsymbol{r}_i$ is a vector tangent to the trajectory of points A_i, A_{i1} and A_{i2}. It verifies $\left\| \boldsymbol{r}_i \right\| = L$

$\boldsymbol{e}_{ij}$ is the vector joining D to B_{ij}

$\boldsymbol{d}_{ij}$ the vector joining the end point C to B_{ij}

ω_x, ω_y and ω_z are angular velocities of half moving platform {3-4} (upper part in Figure 11) relatively to the ground

$\dot{\varepsilon}$ the angular velocity of half travelling plate {1-2} (lower part) relatively to travelling plate's part 3-4 about $\boldsymbol{v}_1$.

Next step of the method consists in doing elementary operations on this system (which do not affect the rank of the system) to end up with the following system:

$$\begin{bmatrix} \boldsymbol{J}_q \\ \boldsymbol{0} \end{bmatrix} \dot{\boldsymbol{q}} = \begin{bmatrix} \boldsymbol{J}_x & \boldsymbol{J}_{int}^{x} \\ \boldsymbol{0} & \boldsymbol{J}_{int} \end{bmatrix} \begin{bmatrix} \dot{\boldsymbol{x}} \\ \boldsymbol{v}_{int} \end{bmatrix} \tag{23}$$

where $\boldsymbol{J}_{int}$ and $\boldsymbol{J}_{int}^{x}$ are 4×4 matrices and $\boldsymbol{v}_{int}$ is a velocity vector. This system has the particularity of being triangular by blocs. In this particular case, multiplying both parts of the system with the following invertible matrix:

$$\boldsymbol{M} = \begin{bmatrix} \frac{1}{2} & \frac{1}{2} & 0 & 0 & 0 & 0 & 0 & 0 \\ 0 & 0 & \frac{1}{2} & \frac{1}{2} & 0 & 0 & 0 & 0 \\ 0 & 0 & 0 & 0 & \frac{1}{2} & \frac{1}{2} & 0 & 0 \\ 0 & 0 & 0 & 0 & 0 & 0 & \frac{1}{2} & \frac{1}{2} \\ 1 & -1 & 0 & 0 & 0 & 0 & 0 & 0 \\ 0 & 0 & 1 & -1 & 0 & 0 & 0 & 0 \\ 0 & 0 & 0 & 0 & 1 & -1 & 0 & 0 \\ 0 & 0 & 0 & 0 & 0 & 0 & 1 & -1 \end{bmatrix} \qquad (\det(\boldsymbol{M}) = 1) \tag{24}$$

and taking into account the fact that rods $i1$ and $i2$ are parallel, in working situation, leads to such a system. The results are:

$$\boldsymbol{J_q} = \begin{bmatrix} \boldsymbol{r_1}.\boldsymbol{l_1} & 0 & 0 & 0 \\ 0 & \boldsymbol{r_2}.\boldsymbol{l_2} & 0 & 0 \\ 0 & 0 & \boldsymbol{r_3}.\boldsymbol{l_3} & 0 \\ 0 & 0 & 0 & \boldsymbol{r_4}.\boldsymbol{l_4} \end{bmatrix}, \; \boldsymbol{J_x} = \begin{bmatrix} \boldsymbol{l_1}^T & R\boldsymbol{v_1}.\boldsymbol{l_1} \\ \boldsymbol{l_2}^T & R\boldsymbol{v_1}.\boldsymbol{l_2} \\ \boldsymbol{l_3}^T & 0 \\ \boldsymbol{l_4}^T & 0 \end{bmatrix}, \tag{25}$$

$$\boldsymbol{J_{int}^x} = \begin{bmatrix} [\boldsymbol{e_1}\times\boldsymbol{l_1}]^T & (\boldsymbol{v_1}\times\boldsymbol{d_1}).\boldsymbol{l_1} \\ [\boldsymbol{e_2}\times\boldsymbol{l_2}]^T & (\boldsymbol{v_1}\times\boldsymbol{d_2}).\boldsymbol{l_2} \\ [\boldsymbol{e_3}\times\boldsymbol{l_3}]^T & 0 \\ [\boldsymbol{e_4}\times\boldsymbol{l_4}]^T & 0 \end{bmatrix}, \qquad \boldsymbol{J_{int}} = \begin{bmatrix} [\boldsymbol{f_1}\times\boldsymbol{l_1}]^T & (\boldsymbol{v_1}\times\boldsymbol{f_1}).\boldsymbol{l_1} \\ [\boldsymbol{f_2}\times\boldsymbol{l_2}]^T & (\boldsymbol{v_1}\times\boldsymbol{f_2}).\boldsymbol{l_2} \\ [\boldsymbol{f_3}\times\boldsymbol{l_3}]^T & 0 \\ [\boldsymbol{f_4}\times\boldsymbol{l_4}]^T & 0 \end{bmatrix}, \tag{26}$$

and:

$$\boldsymbol{v_{int}} = \begin{bmatrix} \omega_x & \omega_y & \omega_z & \dot{\varepsilon} \end{bmatrix}^T \tag{27}$$

($\boldsymbol{e_i}$ is the vector joining D to B_i, $\boldsymbol{d_i}$ the one linking C to B_i, $\boldsymbol{f_i}$ is the vector linking B_{i1} to B_{i2}: $\boldsymbol{f_i} = \boldsymbol{e_{i2}} - \boldsymbol{e_{i1}}$.)

$\boldsymbol{J_{int}}$ will witness of – what we call – "internal singularities". In fact, if $\boldsymbol{J_{int}}$ is not singular, (23) implies that:

$$\boldsymbol{v_{int}} = \boldsymbol{0} \tag{28}$$

which means that half-travelling plate {3-4} keeps always the same orientation ($\omega_x = \omega_y = \omega_z = 0$) and it is the same for part {1-2} while $\dot{\varepsilon} = 0$.

Furthermore, relation:

$$\boldsymbol{J_q}\,\dot{\boldsymbol{q}} = \boldsymbol{J_x}\,\dot{\boldsymbol{x}} + \boldsymbol{J_{int}^x}\,\boldsymbol{v_{int}}. \tag{29}$$

derived from (23) falls into the usual velocity relationship (19).

Verifying $\boldsymbol{J_{int}}$ is not singular can be done by computing its determinant.

It leads to the particular following relationship:

$$\Big(\big((\boldsymbol{f_1}\times\boldsymbol{l_1})\times(\boldsymbol{f_2}\times\boldsymbol{l_2})\big)\times\big((\boldsymbol{f_3}\times\boldsymbol{l_3})\times(\boldsymbol{f_4}\times\boldsymbol{l_4})\big)\Big).\boldsymbol{e_x} \neq 0 \tag{30}$$

By verifying that this relation is always true in the whole workspace we can guarantee that no "internal" singularity occurs. For other type of singularities, usual Jacobean matrices need to be studied: $\boldsymbol{J_q}$ will enlighten "under-mobilities" and $\boldsymbol{J_x}$, "over-mobilities".

4.3.3 Modelling for the over-constrained case

This modelling considers the linear guide as a pure, one-dof, prismatic joint. It implies that the travelling plate is a subset with only 7 dof, and the system must be rewritten without considering terms associated to $\dot{\varepsilon}$. As a consequence, $\boldsymbol{J_{int}}$ and $\boldsymbol{J_{int}^x}$ are 4×3 matrixes:

$$\boldsymbol{J_{int}^x} = \begin{bmatrix} [\boldsymbol{e_1}\times\boldsymbol{l_1}]^T \\ [\boldsymbol{e_2}\times\boldsymbol{l_2}]^T \\ [\boldsymbol{e_3}\times\boldsymbol{l_3}]^T \\ [\boldsymbol{e_4}\times\boldsymbol{l_4}]^T \end{bmatrix}, \; \boldsymbol{J_{int}} = \begin{bmatrix} [\boldsymbol{f_1}\times\boldsymbol{l_1}]^T \\ [\boldsymbol{f_2}\times\boldsymbol{l_2}]^T \\ [\boldsymbol{f_3}\times\boldsymbol{l_3}]^T \\ [\boldsymbol{f_4}\times\boldsymbol{l_4}]^T \end{bmatrix}. \tag{31}$$

The fact that the system gets over-determined (more equations than unknowns) reveals the over-constraint of the mechanism. To make sure the mechanism doesn't show "internal" singularities, we must guarantee that $\boldsymbol{J_{int}}$ is always of full rank ($\mathrm{rank}(\boldsymbol{J_{int}}) = 3$). Considering the symmetrical role of the 4 spatial parallelograms, we obtain the mathematical relation revealing "internal" singularities by developing arbitrary one of the four 3×3 determinant D_{ijk} of this matrix:

$$D_{ijk} = \det\left(\begin{bmatrix} [\boldsymbol{f_i}\times\boldsymbol{l_i}]^T \\ [\boldsymbol{f_j}\times\boldsymbol{l_j}]^T \\ [\boldsymbol{f_k}\times\boldsymbol{l_k}]^T \end{bmatrix}\right) \tag{32}$$

$$D_{ijk} = \big((\boldsymbol{l_i}\times\boldsymbol{l_j}).\boldsymbol{f_i}\big)\big((\boldsymbol{f_j}\times\boldsymbol{f_k}).\boldsymbol{l_k}\big) - \big((\boldsymbol{f_i}\times\boldsymbol{f_j}).\boldsymbol{l_i}\big)\big((\boldsymbol{l_j}\times\boldsymbol{l_k}).\boldsymbol{f_k}\big) \tag{33}$$

for $(i,j,k) \in \{(1,2,3),(1,2,4),(1,3,4),(2,3,4)\}$.

5 Eureka: combining redundancy and T-to-R Transformation

This section of the paper introduces a novel mechanical architecture which combines two of the previous features; Eureka, the proposed machine, is redundant (6 motors for 5 dof provide actuation redundancy) and it is based on a three-part travelling plate with two linear joints. The machine offers 3 translations and 2 rotations with large tilting capabilities in both directions; the first axis of rotation has a constant direction with respect to a fixed frame, the second axis is orthogonal to the first one.

A detailed kinematic analysis is carried out and leads to geometrical conditions to be verified by the mechanism for proper functioning. Then a kinematic modelling illustrates the mechanism simplicity and provides a first evaluation of the machine workspace. Finally, preliminary information is given regarding practical implementation of this new architecture.

5.1 General concept

Eureka, the proposed machine is a 6-actuator / 5-dof parallel mechanism. In Figure 13, a joint-and-loop graph is depicted: P, R, S and U stand for Prismatic, Revolute, Spherical and Universal joints. Grey boxes represent actuated joints; white boxes passive joints. Underlined letter stands for a joint equipped with a position sensor. Circles express a kinematic coupling between two joints.

As for Delta and H4 architectures, the actuators are fixed on the base to reduce moving parts' masses. As for Delta and H4, motors may be rotational or linear, the ball joints may be replaced by U-joints (to get rid of internal motions). One must notice the machine's symmetrical architecture: the machine's upper and lower parts are identically made of a "spatial-parallelogram" and two single rods. Each single rod is connected to "spatial parallelogram".

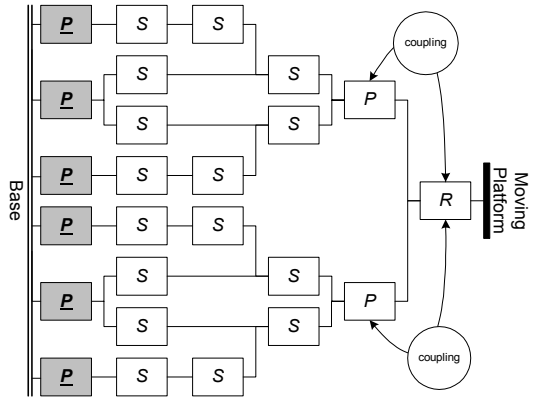

Figure 13. Joint-and-loop graph

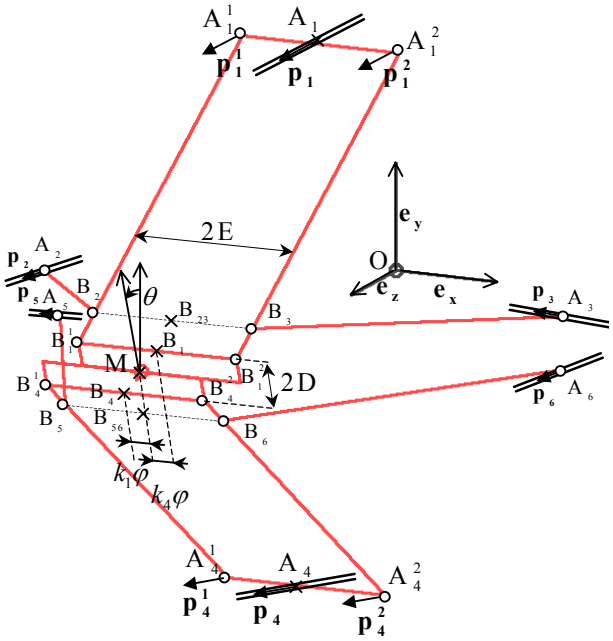

Figure 14. Kinematics scheme

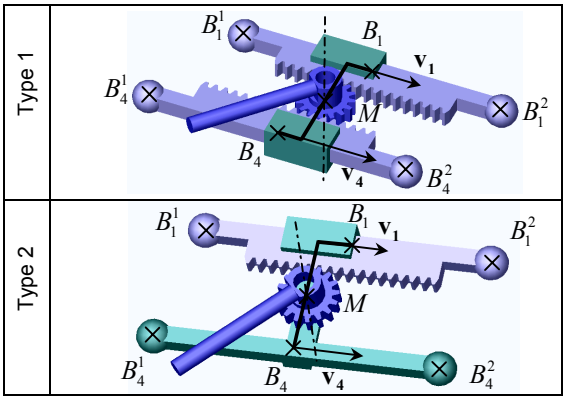

Figure 15. Different types of travelling plates

Note that, in general, the "spatial-parallelogram" chains (that is: **P**$(SS)_2$ chains) implement only one constraint on a mechanism (3 translations and 2 rotations remain feasible); would a "spatial-parallelogram" be made of **P**$R(RR)_2R$ chains (as done on the Orthoglide [23]) it will implement two constraints on a mechanism (3 translations and 1 rotation remain feasible).

The travelling plate is the one introduced in [19] with the I4 robot: while two sub-parts shift relatively one to the other, a mechanical device transforms this motion into a rotation. Two types of travelling plates exist (see Figure 15): Type 1 is made of two prismatic joints and two kinematically coupled rack-and-pinion systems. Type 2 is made up with one part less, but looses Type 1 symmetrical design (good for balancing load among the parts).

5.2 Workspace analysis

In this paper the focus is put on one particular design, where six linear motors are all directed by $\mathbf{e}_z$: this guarantees a large workspace in this particular direction. The selected geometrical parameters are as follows $H = 0.45$ m, $I = 0.08$ m and $J = 0.4$ m. The travelling plate is of type 1. Geometrical parameters' values are: $D = 0.05$ m, $E = 0.06$ m and $k_1 = -0.05$ m/rad. Note that the amplification ratio $|k_1|$ is chosen equal to D in order to have same rotations capabilities for θ and φ. Length of rods is: $l_i = 0.9$ m, $i \in \{1,\ldots,6\}$. Actuators limits are: $0 \le q_i \le 1.26$ m. Figure 17 presents the domain where the condition number of the normalized Jacobean matrix is smaller than 8 (note that along z direction, the workspace is only limited by the actuators' range).

5.3 Practical design considerations

In principle, it could be interesting for simplicity to directly connect the "single rods" to the travelling plate; however, such a practical design faces too many self-collisions. The machine depicted in Figure 16-left shows such a practical design. Another architecture avoiding self-collisions is shown in Figure 16-right. In this case $f = 0$, but single rods have a curved shape.

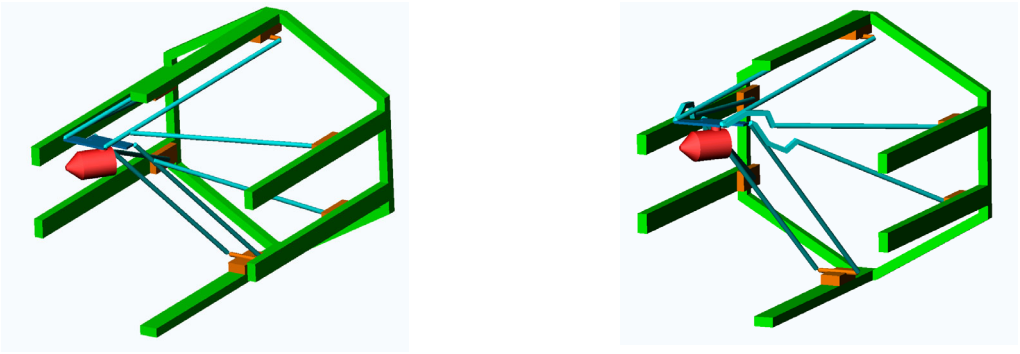

Figure 16. Self-collision-free design #1 and #2

A prototype is about to be built. The practical design is extremely simple thanks to Linear motors (Figure 18). Dimensions are the ones introduced for computing the workspace. Rods and travelling plate are made of aluminium. Spherical joints are new passive joints made by Ephaist Company (Japan). Instead of using rack-and-pinion systems, the mobile platform has been equipped with cable-pulley devices.

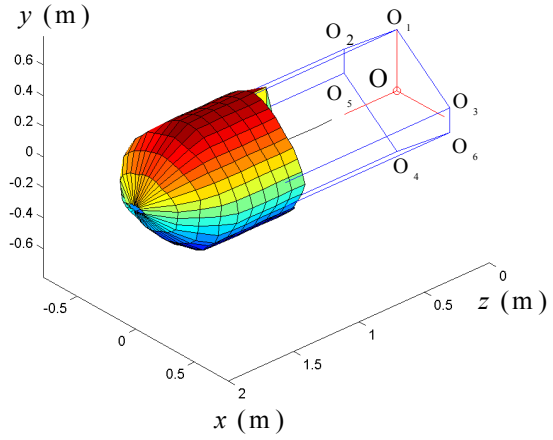

Figure 17. Workspace for cond($\mathbf{J}_q^{-1}\,\mathbf{J}_x\,\mathbf{W}_x^{-1}$) < 8

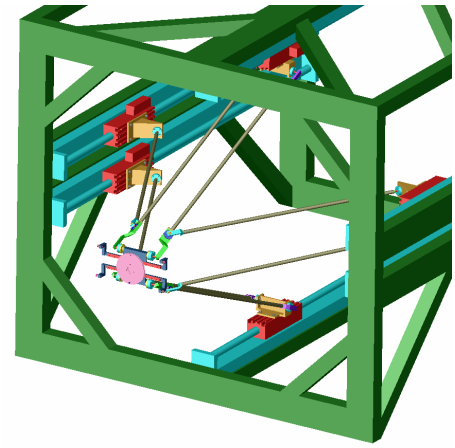

Figure 18. CAD View of the Eureka prototype

6 Conclusion

In this paper, several techniques for reaching high tilting angles have been presented, with a focus on solutions related to articulated travelling plates. Even though such results are still in an early stage of development, they show it might be possible to use, on the one hand, travelling plates embedding passive joints which allows local motion amplification, and on the other hand, actuation redundancy as a way to overcome some singular positions that usually limit the range of motion.

7 References

[1] R. Clavel, "Une nouvelle structure de manipulateur parallèle pour la robotique légère", APII, 23(6), 1985, pp. 371-386.
[2] Rolland L., "The Manta and the Kanuk: Novel 4 dof parallel mechanism for industrial handling", in Proc. of ASME Dynamic Systems and Control Division IMECE'99 Conference, Nashville, November 14-19, 1999, vol. 67, pp 831-844.
[3] Pierrot F., Company O., "H4: a new family of 4-dof parallel robots", in Proc of IEEE/ASME International Conference on Advanced Intelligent Mechatronics, Atlanta, Georgia, USA, September 19-22, 1999, pp. 508-513.
[4] Angeles J., Morozov A., Navarro O., "A novel manipulator architecture for the production of SCARA motions", in Proc. IEEE International Conference on Robotics and Automation, San Francisco, April 24-28, 2000, pp. 2370-2375.
[5] Koevermans W.P. et al., "Design and performance of the four dof motion system of the NLR research flight simulator", in Proc. of AGARD Conf., No 198, Flight Simulation, La Haye, 20-23 October 1975, pp. 17-1/17-11.
[6] Reboulet C. et al, "Rapport d'avancement projet VAP", thème 7, phase 3. Rapport de Recherche 7743, CNES/DERA, January 1991.
[7] Krut S., Company O., Benoit M., Ota H. and Pierrot F., "I4: A new parallel mechanism for Scara motions", in Proc. of IEEE ICRA: Int. Conf. on Robotics and Automation, Taipei, Taiwan, September 14-19, 2003.
[8] Zlatanov D., Fenton R.G., and Benhabib B., "Identification and classification of the singular configurations of mechanisms", Mechanism and Machine Theory, Vol. 33, No. 6, pp. 743-760, August 1998.
[9] Furuya N., Soma K., Chin E., Makino, "Research and development of selective compliance assembly robot arm. II. Hardware and software of SCARA controller", Journal of the Japan Society of Precision Engineering/Seimitsu Kogaku Kaishi, Vol. 49, n°7, 1983, pp. 835-841.
[10] Merlet J.-P. and Pierrot F., "Modélisation des robots parallèles", in Analyse et modélisation des robots manipulateurs, Lavoisier, ISBN 2-7462-0300-6, 2001, pp. 93-144.
[11] Company O., Pierrot F., "A new 3T-1R parallel robot", in Proc. of 9th International Conference on Advanced Robotics, Tokyo, Japan, October 25-27, 1999, pp. 557-562.
[12] Pierrot F., Marquet F., Company O., Gil T., "H4 parallel robot: modeling, design and preliminary experiments", in Proc. of IEEE Int. Conf. On Robotics and Automation, Seoul, Korea, May 2001.
[13] Hervé J.M., "The Lie group of rigid body displacements, a fundamental tool for mechanism design", *Mechanism and Machine Theory*, Vol. 34, 1999, pp. 719-730.
[14] B. Siciliano, "The Tricept Robot: Inverse kinematics, manipulability analysis and closed-loop direct kinematics algorithm", *Robotica*, 1999, pp. 437-445.
[15] C.M. Gosselin, E. St-Pierre and M. Gagné, "On the development of the agile eye: mechanical design, control issues and experimentation", *IEEE Robotics and Automation Society Magazine*, Vol. 3, No. 4, 1996, pp. 29-37.
[16] S.J. Ryu, J.W. Kim, J.C. Hwang, C. Park, H.S. ho, K. Lee, Y. Lee, U. Cornel, F.C. Park and J. Kim, "ECLIPSE: An Overactuated Parallel Mechanism for Rapid Machining", *Proc. ASME Int. Mechanical Engineering Congress and Exposition*, Vol. 8, USA, 1998, pp. 681-689.
[17] F. Marquet, S. Krut, O. Company, F. Pierrot, "Archi, a redundant mechanism for machining with unlimited rotation capacities", *Proc. of ICAR 2001*, Budapest, Hungary, Aug. 2001.
[18] S. Krut, O. Company , F. Marquet, F. Pierrot, "Twice: A Tilting Angle Amplification System for Parallel Robots", *in IEEE Int. Conf. on Robotics and Automation*, Washington, Washington D.C., USA, May 11-15, 2002, pp. 4108-4113.
[19] S. Krut, O. Company, M. Benoit, H. Ota, F. Pierrot, "I4: A New Parallel Mechanism for Scara Motions", *to appear in Proc. of IEEE International Conference on Robotics and Automation*, Taipei, Taiwan, May 2003.
[20] K. Tönshoff, H. Grendel, and R. Kaak, "A hybrid manipulator for laser machining", *in First European-American Forum on Parallel Kinematic Machines*, Milan, Aug. 31-Sept. 1, 1998.
[21] V.B. Zamanov and Z.M. Sotirov, "Parallel manipulators in robotics", *in IMACS/SICE Int. Symp. on Robotics, Mechatronics, and Manufacturing Systems*, Kobe, Sept. 16-20, 1992, pp. 409-418.
[22] L. Stocco and T. Salcudean, "A coarse-fine approach to force-reflecting hand controller design", *in IEEE Int. Conf. on Robotics and Automation*, Minneapolis, April 24-26, 1996, pp. 404-410.
[23] Chablat D. et Wenger Ph, "Design of a Three-Axis Isotropic Parallel Manipulator for Machining Applications: The Orthoglide", Workshop on Fundamental Issues and Future Research Directions for Parallel Mechanisms and Manipulators, October 3-4, Québec, Québec, Canada, 2002.